iScience

CellPress
OPEN ACCESS

Article

Quantum tunneling of hydrogen atom transfer affects mandrel degradation in inertial confinement fusion target fabrication

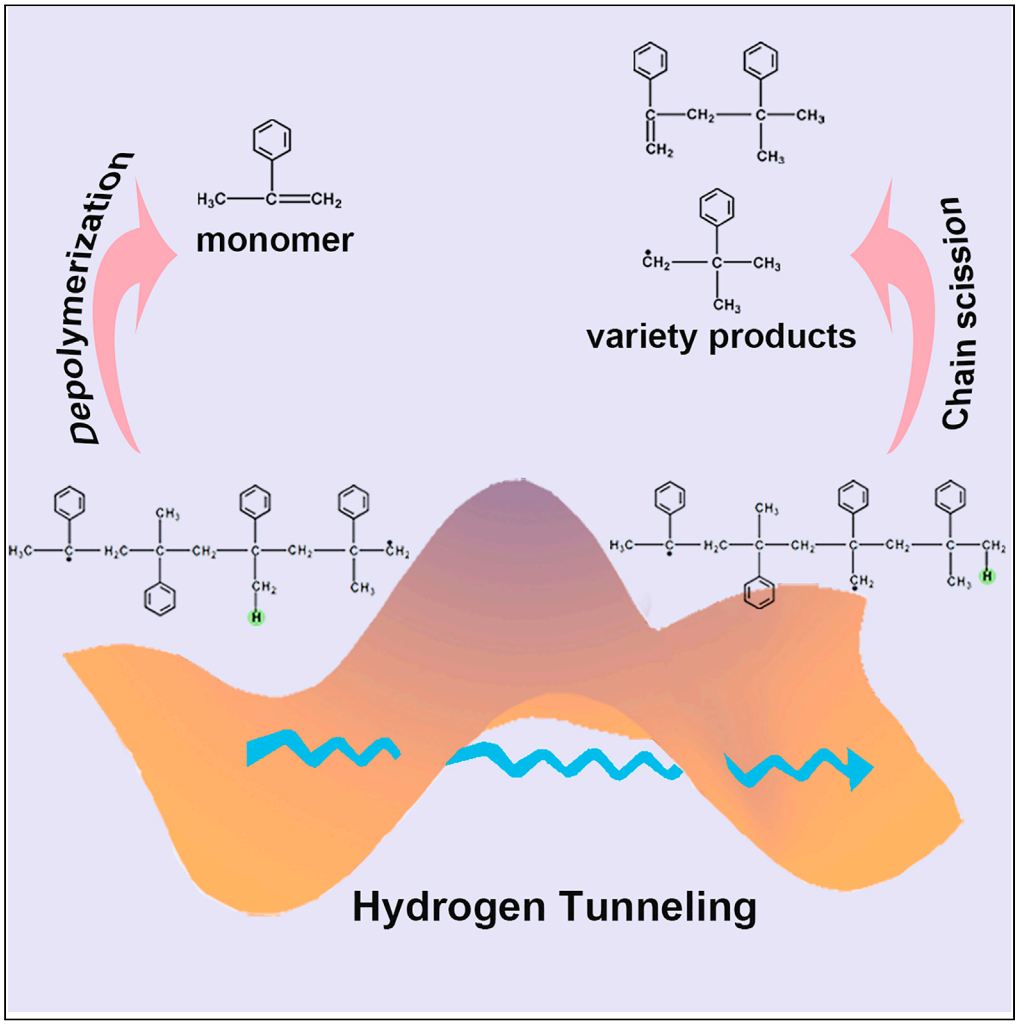

Yu Zhu, Xinrui Yang, Famin Yu, Rui Wang, Qiang Chen, Zhanwen Zhang, Zhigang Wang

bjzzw1973@163.com (Z.Z.)
wangzg@jlu.edu.cn (Z.W.)

Highlights

Tunneling of hydrogen atom transfer (HAT) brings uncertainty to mandrel degradation

Lower energy barrier and stronger tunneling make active-end HAT occur more easily

Chain scission following HAT leads to a variety of products other than monomers

Zhu et al., iScience 25, 103674
January 21, 2022
https://doi.org/10.1016/j.isci.2021.103674

iScience

CellPress
OPEN ACCESS

Article

Quantum tunneling of hydrogen atom transfer affects mandrel degradation in inertial confinement fusion target fabrication

Yu Zhu,[1] Xinrui Yang,[1] Famin Yu,[1] Rui Wang,[1] Qiang Chen,[2] Zhanwen Zhang,[2,*] and Zhigang Wang[1,3,*]

SUMMARY

Poly-α-methylstyrene (PAMS) is considered as the preferred mandrel material, whose degradation is crucial for the fabrication of high-quality inertial confinement fusion (ICF) targets. Herein, we reveal that hydrogen atom transfer (HAT) during PAMS degradation, which is usually attributed to the thermal effect, unexpectedly exhibits a strong high-temperature tunneling effect. Specifically, although the energy barrier of the HAT reaction is only 10^{-2} magnitude different from depolymerization, the tunneling probability of the former can be 14–32 orders of magnitude greater than that of the latter. Furthermore, chain scission following HAT will lead to a variety of products other than monomers. Our work highlights that quantum tunneling may be an important source of uncertainty in PAMS degradation, which will provide a direction for the further development of key technology of target fabricating in ICF research and even the solution of plastic pollution.

INTRODUCTION

Inertial confinement fusion (ICF) (Betti and Hurricane, 2016; Atzeni and Meyer-ter-Vehn, 2004; Lindl, 1998), one of the most promising ways to control thermonuclear fusion reaction, has shown huge potential for the ultimate realization of fusion ignition (Jeff, 2021; Zhang et al., 2020; Edwards et al., 2013). Among the multiple parts of ICF experiments, target is essential, whose quality has an extremely important influence on the reliability and degree of precision for subsequent experimental results (Tucker-Schwartz et al., 2010; Antipa et al., 2013). In recent years, the degradable mandrel technique with poly-α-methylstyrene (PAMS) degradation as the core has become one of the main technologies for fabricating high-quality ICF targets (Letts et al., 1995; Fearon et al., 1997). For this technology, one key problem is how to achieve effective degradation of PAMS. Despite the continuous improvement of the synthesis methods and experimental conditions, the degradation of PAMS, just like the degradation of synthetic plastics, cannot completely occur in accordance with the ideal depolymerization reaction to produce monomer, which brings about the uncertainty of degradation (Brown and Wall, 1958; Poutsma, 2007). Obviously, this issue is not only significant for ICF research but also fundamental to the understanding of mechanisms of environmental pollution caused by common plastics that are also composed of hydrogen and carbon, etc.

Notably, researchers have realized that hydrogen atom transfer (HAT) is a universal reaction during degradation, which will lead to changes in the polymer structure. It has been well accepted that H atom on the main chain of polymers composed of light elements can be seized by free radical to form a new intrachain radical which will cause random chain scission (Poutsma, 2007; Guyot, 1986). In this view, the occurrence of HAT reaction in PAMS may be an important reason that leads to the degradation of PAMS deviating from the ideal depolymerization process. However, although experimental technology (e.g., in situ measurements of spectra) has been greatly improved to study the reaction mechanism (Kalampounias et al., 2003), direct experimental descriptions are still lacking. Moreover, for such a long-distance, HAT process that involves breaking the chemical bond or even overcoming the steric hindrance effect, it is not relatively easy to achieve from the perspective of classical thermal disturbance. Therefore, it is necessary to conduct research on HAT reactions in PAMS at the atomic level based on a new perspective.

Actually, owing to the light mass of the H atom, many processes involving it are susceptible to quantum-mechanical effects, such as tunneling (Bell, 1980; McMahon, 2003; Schreiner, 2017; Mayer, 2011; Meisner

[1]Institute of Atomic and Molecular Physics, Jilin University, Changchun 130012, China

[2]Laser Fusion Research Center, China Academy of Engineering Physics, Mianyang 621900, China

[3]Lead contact

*Correspondence: bjzzw1973@163.com (Z.Z.), wangzg@jlu.edu.cn (Z.W.)

https://doi.org/10.1016/j.isci.2021.103674

and Kästner, 2016). Tunneling by H species is of critical importance for many reactions, such as proton-coupled electron transfer reactions (Hammes-Schiffer, 2001; Glover et al., 2017), redox enzyme reactions (Knapp and Klinman, 2002; Gao and Truhlar, 2002), conformational inversion of molecules (Brunton et al., 1976; Schreiner et al., 2011; Mardyukov et al., 2017; Koch et al., 2017), and rotation of hydrogen bonds (Ranea et al., 2004; Richardson et al., 2016). Generally, tunneling is significant at low temperatures, although H tunneling is not restricted to such temperatures (McMahon, 2003; Schreiner et al., 2011; Mardyukov et al., 2017). These attracted our attention: for PAMS that degrades at temperatures above room temperature, can the tunneling effect in their HAT play a leading role under this temperature condition?

Based on the above, we focus on the HAT reactions in PAMS to study their classical over-barrier process and through-barrier quantum tunneling process based on the high-precision quantum mechanics calculations. Surprisingly, the results show that the strong high-temperature tunneling effect presented in HAT is significant for degradation, which may be an important source of the complexity for degradation problems. These findings contribute to achieving more efficient degradation of PAMS for the fabrication of ICF targets and can provide useful guidance for further understanding the plastic degradation.

RESULTS AND DISCUSSION

Reaction paths of hydrogen atom transfer and depolymerization

Considering the reliability and resource requirements of quantum calculations, the di-radical PAMS tetramer was used, for which the rationality of the structure selection has been confirmed in our previous studies (Zhu et al., 2021; Yu et al., 2015). First, we obtained the possible reaction paths by means of TS optimization and intrinsic reaction coordinate (IRC) analysis. Detailed methods introduction can be seen STAR Methods. The TSs structures and reaction paths can be seen in Figures S1 and S2. Their schematic diagram and corresponding potential energy surfaces (PESs) are shown in Figure 1. For the di-radical structure, there are two kinds of HAT paths at each head end (C-unsaturated end) and tail end (CH_2-unsaturated end). By taking the tail end as an example, due to the steric hindrance of CH_2 in the ortho position, the C atom at the tail end will seize the H atom on the methyl or methylene group of the adjacent monomer. However, because the nearby benzene ring also has steric hindrance, neither reaction is a simple one-step process. At first, this benzene ring will flip to form an intermediate (iso2). There are two cases afterward. In the first case, the C atom at the tail end will directly seize the H atom from the neighboring methyl group ($H_{tra\text{-}ta1}$). In the second case, a "back-biting" process will continue to occur at the tail end, resulting in the formation of a 6-membered ring intermediate (iso3). Subsequently, the H atom from the methylene group on the second monomer (head-end monomer is the first) will be transferred to the tail end ($H_{tra\text{-}ta2}$). These two kinds of HAT reactions were also observed in the dynamic simulations (Figure S3). Similarly, there are two reactions at the head end. The difference is that the H atom on the methyl group of the second monomer can be transferred directly to the head end ($H_{tra\text{-}he1}$), whereas the transfer of the H atom on the methylene ($H_{tra\text{-}he2}$) requires a prerequisite: the polymer must first undergo an isomerization process to form a 5-membered ring intermediate (iso1). The coordinates of the structures in the above reactions can be seen in Table S1.

Classical over-barrier and through-barrier quantum tunneling process

Next, we analyzed these reactions from the perspective of energy (Figure 1B). For three isomerization processes, including the benzene ring flip, "back-biting" of the tail end to form a 6-membered ring, and "back-biting" of the head end to form a 5-membered ring intermediate, their energy barriers are 0.26 eV, 0.24 eV, and 0.23 eV, respectively. This indicates that the isomerization of PAMS easily occurs during degradation, especially the formation of polycyclic intermediates. In the two HAT reactions at the tail end, although the energy barriers for $H_{tra\text{-}ta1}$ and $H_{tra\text{-}ta2}$ are both 0.60 eV, considering that degradation is a reversible reaction, the relative energies of the product and TS (called the reverse energy barrier) also affect the occurrence of the reaction. The greater reverse energy barrier of $H_{tra\text{-}ta2}$ (0.86 eV) than that of $H_{tra\text{-}ta1}$ (0.67 eV) suggests that H atoms on the methylene are more likely to transfer, reflecting the selectivity of the HAT reaction. This rule also applies to $H_{tra\text{-}he1}$ and $H_{tra\text{-}he2}$, for which the corresponding energy barriers of these two reactions are 1.39 eV and 1.25 eV. Additionally, the HAT reaction is more likely to occur at the tail end. In a previous study,[30] we have investigated the depolymerization reactions of PAMS. The energy barriers required for the dissociation of the head and tail end to generate monomer are D_{he} (0.68 eV) and D_{ta} (0.82 eV), respectively. By comparison, it was found that the tail end is more prone to occur HAT rather than depolymerization.

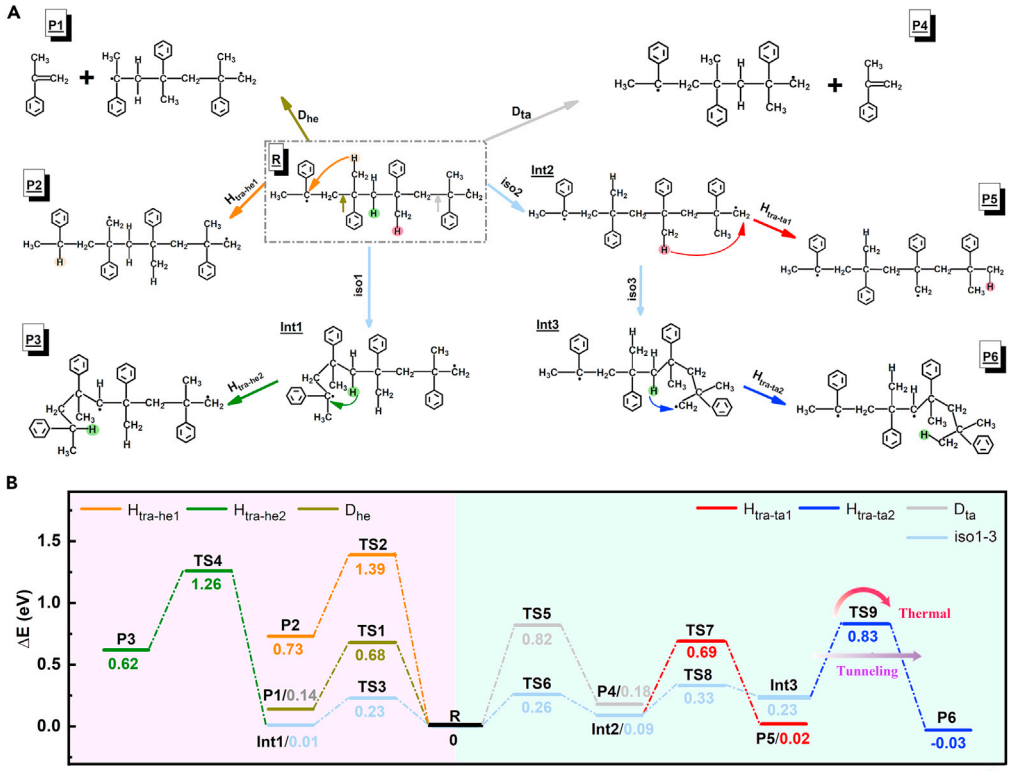

Figure 1. Reaction paths of PAMS

(A) Schematic diagram of reaction paths.

$H_{tra\text{-}he1}$ indicates that the H atom on the methyl group is transferred to the head end (abbreviated as "he," C-unsaturated end). iso1-3 refers to isomerization processes. $H_{tra\text{-}he2}$ represents that the H atom on the methylene is transferred to the head end after occurring iso1. $H_{tra\text{-}ta1}$ indicates that the H atom on the methyl is transferred to the tail end (abbreviated as "ta," CH_2-unsaturated end) after occurring iso2. $H_{tra\text{-}ta2}$ represents that the H atom on the methylene is transferred to the tail end after Int2 occurring iso3. D_{he} and D_{ta} are paths that produce the AMS monomer, which has been studied in our previous work [30].

(B) Potential energy surfaces of these nine reactions. "R," "Int," and "P" represent the reactant, intermediate, and product, respectively. The energy of the reactant is taken as zero. The energy values were all corrected by ZPE. The pink and light blue areas in the figure represent the reaction paths related to the head end and tail end, respectively.

In fact, polymers can not only achieve HAT by overcoming the energy barrier but also instantaneous H transfer through quantum tunneling. Using different excitation energies, we calculated the probabilities of quantum tunneling ($P_{tunneling}$) for PAMS to achieve HAT and monomer dissociation based on the Wentzel–Kramers–Brillouin (WKB) approximation (Wentzel, 1926; Kramers, 1926; Brillouin, 1926). The concise tunneling model and calculation details can be seen in Figure S4 and STAR Methods. Here, the provided energy (E_p) should be higher than the energies of the reactant and product in the reaction, thus giving $P_{tunneling}$, as shown in Figure 2A. With the increase of E_p, $P_{tunneling}$ increases gradually. Since only the high tunneling probability is meaningful, we will not further discuss the low tunneling probability part under the low E_p. When the same excited energy is provided, the $P_{tunneling}$ of tail-end HAT ($H_{tra\text{-}ta1}$ and $H_{tra\text{-}ta2}$), depolymerization (D_{he} and D_{ta}), and head-end HAT ($H_{tra\text{-}he1}$ and $H_{tra\text{-}he2}$) decreases sequentially. The magnitudes of $P_{tunneling}$ for $H_{tra\text{-}he1}$ and $H_{tra\text{-}he2}$ are similar. Considering that the energies of the products for these two reactions are relatively large, the required E_p is also high, thus, we will not discuss their $P_{tunneling}$ in detail later. Moreover, when the E_p is 0.4 eV, the magnitude of $P_{tunneling}$ for $H_{tra\text{-}ta2}$ and $H_{tra\text{-}ta1}$ are 10^{-1} and 10^{-4}, and those for D_{he} and D_{ta} are 10^{-18} and 10^{-33}, showing obvious differences. Therefore, compared with the dissociation of the monomer, the HAT reaction at the tail end has a strong tunneling effect, which can easily occur through tunneling.

Meanwhile, from the classical perspective, the thermal effect will cause the reaction to occur with a certain probability. We further compared the thermal disturbance probability ($P_{thermal}$) and $P_{tunneling}$ by calculating

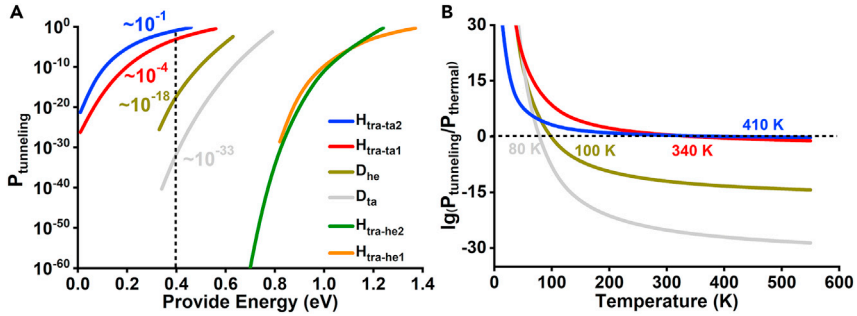

Figure 2. Probabilities of quantum tunneling ($P_{tunneling}$) and thermal disturbance ($P_{thermal}$) of reaction paths

(A) $P_{tunneling}$ as a function of the provided energy (E_p). "~" denotes the magnitude.

(B) Ratio of $P_{tunneling}$ to $P_{thermal}$ of reaction paths when E_p is 0.40 eV. The black dotted line means that the two kinds of probabilities are equal.

the ratios of the two at different temperatures and E_p. Here, to clearly see the difference between $P_{thermal}$ and $P_{tunneling}$, we ignore the possible correlation between the two, which has also been implemented in many researches (Guo et al., 2016; Wang et al., 2021). Figure 2B shows the ratios when the E_p is 0.40 eV. It can be found that the temperatures at which tunneling dominates in $H_{tra\text{-}ta2}$, $H_{tra\text{-}ta1}$, D_{he}, and D_{ta} are approximately 410 K, 340 K, 100 K, and 80 K. This suggests that H tunneling during polymer degradation can play a significant role even at room temperature. Similar laws are also obtained under other E_p (Figures S5 and S6). Actually, it is now well established that H tunneling contributions can be substantial at room temperature (McMahon, 2003; Meisner and Kästner, 2016; Schäfer et al., 2017), but this effect was not previously noticed in polymer degradation. The main role of quantum tunneling in the HAT reaction indicates that PAMS may undergo frequent HAT even at temperatures where degradation does not occur. Moreover, it is worth mentioning that the occurrence of HAT will lead to the change in the structure for the PAMS, resulting in the uncertainty of degradation. Therefore, it can be reasonably speculated that the HAT reaction promoted by quantum tunneling may be an important source of uncertainty in PAMS degradation.

In order to better understand the relevant bond properties, we summarized the bond lengths and bond orders of related C-C bonds in HAT reactions (Table S2). Here, the carbon atom on the group whose hydrogen atom is lost is named as the donor carbon atom. By taking $H_{tra\text{-}ta1}$ as an example, as the H transfer reaction proceeds, the bond length of the C-C bond at the position of the donor C atom is shortened from 1.54 Å to 1.50 Å and the bond orders are enlarged from 1.00 to 1.04, while the bond lengths of its two adjacent C-C bonds are respectively increased from 1.57/1.57 Å to 1.58/1.59 Å, and the bond orders are reduced from 0.97/0.97 to 0.96/0.94. In addition, in all C-C bonds, except for the C–C bond at the monomer linkage site of the head end, these two adjacent C-C bonds are relatively weak, indicating that they are most likely to be broken. The above results indicate that after the H transfer occurs, the C-C bond where the donor C atom is located will be strengthened, and the adjacent C-C bonds will usually be weakened, leading to the occurrence of chain scission at the weaker C-C bond. The other three HAT reactions have similar bond properties (Table S2). Furthermore, we study the chain scission paths after HAT from the perspective of PESs. Also taking $H_{tra\text{-}ta1}$ as an example, there are two possible scission paths after HAT. In the first pathway, a monomer free radical and a chain with a C-unsaturated end are produced. In the second pathway, a dimer and an unsaturated chain form together. The chain scission reactions that occur after the other three HAT reactions also produced various products other than monomers, such as monomer-like, dimer-like, and trimer-like molecules (Figure S7). The analyses of PESs further confirm that HAT contributes to the occurrence of chain scission reactions, thus resulting in the uncertainty of degradation.

Classical kinetic or thermodynamic control is conventionally considered an important way to understand and predict the diversity of chemical reactions. As an increasing number of tunneling phenomena in chemical reactions were revealed, researchers have gradually realized that tunneling control may be regarded as a type of nonclassical kinetic control [17,25]. Moreover, an experimental study of double-hydrogen tunneling in porphycene molecules based on the scanning tunneling microscope (STM) found that the height of the STM tip affects the tunneling properties [27]. Thus, it is conceivable that in future experiments, tunneling can be manipulated through external stimuli, which provides a new idea for regulating the degradation process of PAMS.

Conclusions

In summary, our study revealed the important effect of H atom tunneling on PAMS degradation. The calculation of PESs shows that there are two possible HAT paths at each end of the main chain, namely, the H atom on the methyl or methylene of ortho monomer transfers to the head end and tail end. Among them, for two reactions at the same chain end, the H atom on methylene is more likely to transfer, which reflects the selectivity of the HAT reaction. While, by comparing the energy barriers of reactions at different chain ends, it can be found that HAT occurs more easily at the tail end. More importantly, although the energy barriers required for tail-end HAT and depolymerization differ slightly, their tunneling probabilities are vastly different. At a provided energy of 0.4 eV, the tunneling probability of the former is 14–32 orders of magnitude greater than that of the latter. In particular, the tunneling effect of the former can still dominate at room temperature. Thus, it is known that lower energy barrier and stronger high-temperature tunneling effect result in a reaction in which H atom transfer to the tail end occurs more easily. Additionally, HAT will further promote the occurrence of chain scission to form products other than monomers, thus bringing about the uncertainty of degradation. The above results reveal that tunneling is an important source of the complexity of PAMS degradation, which will provide a guide to control the PAMS degradation for the better fabrication of ICF target. Meanwhile, this study will bring useful insights into solutions to the environmental pollution caused by the incomplete degradation of plastics.

Limitations of the study

This study reveals that high-temperature tunneling may be an important source of uncertainty in the degradation of polymers containing hydrogen and carbon elements. Considering the negative correlation between tunneling and atomic mass, it limits the extension of this conclusion to polymers composed of other elements to a certain extent. Hence, the effect of tunneling on the degradation of a wide range of polymer systems remains to be explored in future research.

STAR★METHODS

Detailed methods are provided in the online version of this paper and include the following:

- KEY RESOURCES TABLE
- RESOURCE AVAILABILITY
  - Lead contact
  - Materials availability
  - Data and code availability
- METHOD DETAILS
  - DFT calculations
  - Dynamic simulation
  - Tunneling and thermal disturbance probabilities
- QUANTIFICATION AND STATISTICAL ANALYSIS

SUPPLEMENTAL INFORMATION

Supplemental information can be found online at https://doi.org/10.1016/j.isci.2021.103674.

ACKNOWLEDGMENTS

This work was supported by the National Natural Science Foundation of China (grant numbers 11974136 and 11674123). Z.W. also acknowledges the assistance of the High-Performance Computing Center of Jilin University and National Supercomputing Center in Shanghai.

AUTHOR CONTRIBUTIONS

Y. Zhu performed simulations and calculations; Z. Wang initiated and designed the work; Z. Wang and Z. Zhang supervised the work; Y. Zhu, X. Yang, F. Yu, R. Wang, Q. Chen, Z. Zhang, and Z. Wang analyzed the data; Y. Zhu, Z. Zhang and Z. Wang wrote the article.

DECLARATION OF INTERESTS

The authors declare no competing interests.

Received: October 26, 2021
Revised: November 16, 2021
Accepted: December 17, 2021
Published: January 21, 2022

REFERENCES

Antipa, N.A., Baxamusa, S.H., Buice, E.S., Conder, A.D., Emerich, M.N., Flegel, M.S., Heinbockel, C.L., Horner, J.B., Fair, J.E., Kegelmeyer, L.M., et al. (2013). Automated ICF capsule characterization using confocal surface profilometry. Fusion Sci. Technol. *63*, 151–159.

Atzeni, S., and Meyer-ter-Vehn, J. (2004). The Physics of Inertial Fusion: Beam Plasma Interaction, Hydrodynamics, Hot Dense Mater (Clarendon Press).

Becke, D.A. (1993). Density-functional thermochemistry. III. The role of exact exchange. J. Chem. Phys. *98*, 5648–5652.

Bell, R.P. (1980). The Tunnel Effect in Chemistry (Chapman & Hall).

Beno, B.R., Fennen, J., Houk, K.N., Lindner, H.J.r., and Hafner, K. (1998). Sigmatropic rearrangement. DFT prediction of a diradi-cal mechanism for a woodward? Hoffmann "allowed" thermal pericyclic reaction. J. Am. Chem. Soc. *120*, 10490–10493.

Betti, R., and Hurricane, O.A. (2016). Inertial-confinement fusion with lasers. Nat. Phys. *12*, 435–448.

Brillouin, L. (1926). La mécanique ondulatoire de Schrödinger; une méthode générale de résolution par approximations successives. Compt. Rend. Hebd. Seances Acad. Sci. *183*, 24.

Brown, D.W., and Wall, L.A. (1958). The pyrolysis of poly-α-methylstyrene. J. Phys. Chem. *62*, 848–852.

Brunton, G., Griller, D.L., Barclay, R.C., and Ingold, K.U. (1976). Kinetic applications of electron paramagnetic resonance spectrosco-py. 26. Quantum-mechanical tunneling in the isomerization of steri-cally hindered aryl radicals. J. Am. Chem. Soc. *98*, 6803–6811.

Edwards, M.J., Patel, P.K., Lindl, J.D., Atherton, L.J., Glenzer, S.H., Haan, S.W., Kilkenny, J.D., Landen, O.L., Moses, E.I., Nikroo, A., et al. (2013). Progress towards ignition on the national igni-tion facility. Phys. Plasmas *20*, 070501.

Elstner, D.P.M., Jungnickel, G., Elsner, J., Haugk, M., Frauenheim, T., Suhai, S., and Seifert, G. (1998). Self-consistent-charge density-functional tight-binding method for simulations of complex materi-als properties. Phys. Rev. B *58*, 7260.

Elstner, M., Frauenheim, T., and Suhai, S. (2003). An approximate DFT method for QM/MM simulations of biological structures and processes. J. Mol. Struct. Theochem. *632*, 29–41.

Fearon, E.M., Letts, S.A., Allison, L.M., and Cook, R.C. (1997). Adapting the decomposable mandrel technique to build specialty ICF targets. Fusion Technol. *31*, 406–410.

Frisch, M.J., Trucks, G.W., Schlegel, H.B., Scuseria, G.E., Robb, M.A., Cheeseman, J.R., Scalmani, G., Barone, V., Mennucci, B., Petersson, G.A., et al. (2009). Gaussian 09, Revision D.01 (Wallingford CT: Gaussian Inc.).

Fukui, K. (1970). Formulation of the reaction coordinate. J. Phys. Chem. *74*, 4161–4163.

Gao, J., and Truhlar, D.G. (2002). Quantum mechanical methods for enzyme kinetics. Annu. Rev. Phys. Chem. *53*, 467–505.

Glover, S.D., Parada, G.A., Markle, T.F., Ott, S., and Ham-marström, L. (2017). Isolating the effects of the proton tunneling distance on proton-coupled electron transfer in a series of homologous tyrosine-base model compounds. J. Am. Chem. Soc. *139*, 2090–2101.

Gonzalez, C., and Schlegel, H.B. (1990). Reaction path following in mass-weighted internal coordinates. J. Phys. Chem. *94*, 5523–5527.

Griffiths, D.J. (2005). Introduction to Quantum Mechanics, Second Edition (Pearson Prentice Hall).

Grimme, S., Antony, J., Ehrlich, S., and Krieg, H. (2010). A consistent and accurate ab initio parametrization of density functional dispersion correction (DFT-D) for the 94 elements H-Pu. J. Chem. Phys. *132*, 154104.

Guo, J., Lü, J.T., Feng, Y.X., Chen, J., Peng, J.B., Lin, Z.R., Meng, X.Z., Wang, Z.C., Li, X.Z., Wang, E.G., and Jiang, Y. (2016). Nu-clear quantum effects of hydrogen bonds probed by tip-enhanced inelastic electron tunneling. Science *352*, 321.

Guyot, A. (1986). Recent developments in the thermal degradation of polystyrene—a review. Polym. Degrad. Stab. *15*, 219–235.

Hammes-Schiffer, S. (2001). Theoretical perspectives on proton-coupled electron transfer reactions. Acc. Chem. Res. *34*, 273–281.

He, X.F., Li, Z., Hu, H.H., Chen, J.W., Zeng, L.Z., Zhang, J.Z., Lin, W.B., and Wang, C. (2021). Chemical looping conversion of ethane to ethanol via photo-assisted nitration of ethane. Cell Rep. Phys. Sci. *2*, 100481.

Hourahine, B., Aradi, B., Blum, V., Bonafé, F., Buccheri, A., Camacho, C., Cevallos, C., Deshaye, M.Y., Dumitrică, T., Dominguez, A., et al. (2020). DFTB+, a software package for efficient approximate density functional theory based atomistic simulations. J. Chem. Phys. *152*, 124101.

Jeff, T. (2021). US achieves laser-fusion record: what it means for nuclear-weapons research. Nature. https://doi.org/10.1038/d41586-021-02338-4.

Kalampounias, A.G., Andrikopoulos, K.S., and Yannopou-los, S.N. (2003). Probing the sulfur polymerization transition in situ with Raman spectroscopy. J. Chem. Phys. *118*, 8460–8467.

Knapp, M.J., and Klinman, J.P. (2002). Environmentally coupled hydrogen tunneling. Eur. J. Biochem. *269*, 3113–3121.

Koch, M., Pagan, M., Persson, M., Gawinkowski, S., Waluk, J., and Kumagai, T. (2017). Direct observation of double hydrogen transfer via quantum tunneling in a single porphycene molecule on a Ag(110) surface. J. Am. Chem. Soc. *139*, 12681–12687.

Kramers, H.A. (1926). Wellenmechanik und halbzahlige Quan-tisierung. Z. für Phys. *39*, 828.

Krüger, T., Elstner, M., Schiffels, P., and Frauenheim, T. (2005). Validation of the density-functional based tight-binding approximation method for the calculation of reaction energies and other data. J. Chem. Phys. *122*, 114110.

Landau, L.D., and Lifshitz, E.M. (1980). Statistical Physics Part 1 (Pergamon Press).

Lee, C., Yang, W., and Parr, R.G. (1988). Development of the Colle-Salvetti correlation-energy formula into a functional of the electron density. Phys. Rev. B: Condens. Matter Mater. Phys. *37*, 785–789.

Letts S.A., Fearon E., Allison L., Buckley S., Saculla M., Cook R. (1995). Decomposable mandrel project. (Progress report: United States). https://digital.library.unt.edu/ark:/67531/metadc778710/m2/1/high_res_d/85915.pdf.

Lindl, J.D. (1998). Inertial Confinement Fusion: The Quest for Ignition and Energy Gain Using Indirect Drive (Springer Verlag).

Lyuben, Z., Thomas, H., Serguei, P., Gotthard, S., and Duarte, H.A. (2005). An efficient a posteriori treatment for dispersion interaction in density-functional-based tight binding. J. Chem. Theory. Comp. *1*, 841.

Mardyukov, A., Quanz, H., and Schreiner, P.R. (2017). Conformer-specific hydrogen atom tunneling in trifluoromethylhydroxycarbene. Nat. Chem. *9*, 71–76.

Martyna, G.J., Tuckerman, M.E., Tobias, D.J., and Klein, M.L. (1996). Explicit reversible integrators for extended systems dynamics. Mol. Phys. *87*, 1117–1157.

Mayer, J.M. (2011). Understanding hydrogen atom transfer: from bond strengths to Marcus theory. Acc. Chem. Res. *44*, 36–46.

McMahon, R.J. (2003). Chemical reactions involving quantum tunneling. Science *299*, 833.

Meisner, J., and Kästner, J. (2016). Atom tunneling in chemistry. Angew. Chem. Int. Ed. *55*, 5400–5413.

Niu, S., and Hall, M.B. (2000). Theoretical studies on reactions of transition-metal complexes. Chem. Rev. *100*, 353–406.

Poutsma, M.L. (2007). Mechanistic analysis and thermochemical kinetic simulation of the products from pyrolysis of poly(α-methylstyrene), especially the unrecognized role of phenyl shift. J. Anal. Appl. Pyrolysis *80*, 439–452.

Ranea, V.A., Michaelides, A., Ramirez, R., de Andres, P.L., Verges, J.A., and King, D.A. (2004). Water dimer diffusion on Pd{111} assisted by an H-bond donor-acceptor tunneling exchange. Phys. Rev. Lett. *92*, 136104.

Rappe, A.K., Casewit, C.J., Colwell, K.S., Goddard, W.A., and Skiff, W.M. (1992). UFF, a full periodic table force field for molecular mechanics and molecular dynamics simulations. J. Am. Chem. Soc. *114*, 10024–10035.

Richardson, J.O., Pérez, C., Lobsiger, S., Peid, A.A., Temelso, B., Shields, G.C., Kisiel, Z., Wales, D.J., Pate, B.H., and Althorpe, S.C. (2016). Concerted hydrogen-bond breaking by quantum tunneling in the water hexamer prism. Science *351*, 1310.

Schäfer, M., Peckelsen, K., Paul, M., Martens, J., Oomens, J., Berden, G., Berkessel, A., and MeijerBrillouin, A.J.H.M. (2017). Hydrogen tunneling above room temperature evidenced by infrared ion spectroscopy. J. Am. Chem. Soc. *139*, 5779–5786.

Schreiner, P.R. (2017). Tunneling control of chemical reactions: the third reactivity paradigm. J. Am. Chem. Soc. *139*, 15276–15283.

Schreiner, P.R., Reisenauer, H.P., Ley, D., Gerbig, D., Wu, C.H., and Allen, W.D. (2011). Methylhydroxycarbene: tunneling control of a chemical reaction. Science *332*, 1300.

Siebert, M.R. (2010). Differentiating mechanistic possibilities for the thermal, intramolecular [2 + 2] cycloaddition of Allene−Ynes. J. Am. Chem. Soc. *132*, 11952–11966.

Takano, Y., Kubo, S., Onishi, T., Isobe, H., Yoshioka, Y., and Yamaguchi, K. (2001). Theoretical studies on the magnetic interaction and reversible dioxygen binding of the active site in hemocyanin. Chem. Phys. Lett. *335*, 395–403.

Tucker-Schwartz, A.K., Bei, Z.M., Garrell, R.L., and Jones, T.B. (2010). Polymerization of electric field-centered double emulsion droplets to create polyacrylate shells. Langmuir *26*, 18606–18611.

Wang, H., Yao, Y.S., Peng, F., Liu, H.Y., and Hemley, R.J. (2021). Quantum and classical proton diffusion in superconducting clathrate hydrides. Phys. Rev. Lett. *126*, 117002.

Wentzel, G. (1926). Eine Verallgemeinerung derQuantenbed-ingungen für die Zwecke der Wellenmechanik. Z. für Phys. *38*, 518.

Yamaguchi, K., Jensen, F., Dorigo, A., and Houk, K.N. (1988). A spin correction procedure for unrestricted Hartree-Fock and Møller-Plesset wavefunctions for singlet diradicals and polyradicals. Chem. Phys. Lett. *149*, 537–542.

Yu, Z.X., Caramella, P., and Houk, K.N. (2003). Dimerizations of nitrile oxides to furoxans are stepwise via dinitrosoalkene diradi-cals:? A density functional theory study. J. Am. Chem. Soc. *125*, 15420–15425.

Yu, T.R., Gao, Y., Wang, B., Dai, X., Jiang, W.R., Song, R.X., Zhang, Z.W., Jin, M.X., Tang, Y.J., and Wang, Z.G. (2015). Depolymer-ization of free-radical polymers with spin migrations. Chemphyschem. *16*, 3308–3312.

Zhang, F., Cai, H.B., Zhou, W.M., Dai, Z.S., Shan, L.Q., Xu, H., Chen, J.B., Ge, F.J., Tang, Q., Zhang, W.S., et al. (2020). Enhanced energy coupling for indirect-drive fast-ignition fusion targets. Nat. Phys. *16*, 810–814.

Zhang, H., Novak, A.J.E., Jamieson, C.S., Xue, X.S., Chen, S.M., Trauner, D., and Houk, K.N. (2021). Computational Exploration of the Mechanism of Critical Steps in the biomimetic synthesis of preuisolactone A, and discovery of new ambimodal (5 + 2)/(4 + 2) cycloadditions. J. Am. Chem. Soc. *143*, 6601–6608.

Zhu, Y., Liu, Z., Yu, F.M., Chen, Q., Feng, W., Zhang, Z.W., and Wang, Z.G. (2021). Mandrel degradation model of combined fast and slow processes. High Power Laser Sci. Eng. *9*, e1.

Ziegler, T., and Autschbach, J. (2005). Theoretical methods of poten-tial use for studies of inorganic reaction mechanisms. Chem. Rev. *105*, 2695–2722.

STAR★METHODS

KEY RESOURCES TABLE

REAGENT or RESOURCE	SOURCE	IDENTIFIER
Software and algorithms		
Gaussian 09	http://gaussian.com/	N/A
DFTB+19.1	https://dftbplus.org/about-dftb/	N/A

RESOURCE AVAILABILITY

Lead contact

Further information and requests for resources should be directed to and will be fulfilled by the lead contact, Z.G. Wang (wangzg@jlu.edu.cn).

Materials availability

This study did not generate new reagents.

Data and code availability

Data - Data reported in this paper will be shared by the lead contact upon request.

Code - No new code was generated during the course of this study.

Other - Any additional information required to reanalyze the data reported in this paper is available from the lead contact upon request.

METHOD DETAILS

DFT calculations

To carry out this study, the 3rd generation dispersion (Grimme et al., 2010) corrected density functional theory (DFT-D3) of first-principles was used to investigate the reaction paths. All structures (including reactants, transition states (TSs) and products) were fully optimized at the B3LYP-D3 (Lee et al., 1988; Becke, 1993) level in conjunction with 6-31+G(d,p) basis sets. B3LYP is a commonly used functional for studying di-radical systems, which can produce reasonable energetic results for di-radical intermediates and transition states (Beno et al., 1998; Yu et al., 2003; Siebert, 2010). Based on the optimized geometries, the nature of extreme points was evaluated by performing harmonic vibrational frequency calculations. The numbers of imaginary frequencies were used to confirm that the structure was a stable point or TS. Meanwhile, the zero-point energy (ZPE) scaled by the ZPE scaling factor was also determined. The IRC (Fukui, 1970; Gonzalez and Schlegel, 1990) was calculated to ensure the reliability of the reaction process. Due to the existence of spin contamination in the low-spin state, we corrected it with an approximate spin-projection (AP) method. AP is an effective way to eliminate spin contamination from the broken-symmetry (BS) solution (Yamaguchi et al., 1988; Takano et al., 2001). According to this scheme, the energies of the pure singlet (E_S) is given below:

$$E_S = E_{BS} + \frac{<S^2>_{BS}}{<S^2>_T - <S^2>_{BS}}(E_{BS} - E_T)$$

Among them, E_{BS} and E_T represent the energies of broken-symmetry state and triplet state. $<S^2>_{BS}$ and $<S^2>_T$ are spin eigenvalues of broken-symmetry state and triplet state. No atoms are frozen and no symmetry restrictions are imposed in all calculations. The above calculations were all performed using the Gaussian 09 package (Frisch et al., 2009).

Dynamic simulation

For the dynamic simulation, the DFTB+19.1 package (Hourahine et al., 2020) was used based on the empirical dispersion corrected density functional tight-binding (DFTB-D) method (Elstner et al., 1998, 2003). For systems selected in this paper, we chose the Slater-Koster type parameters (Elstner et al., 1998), which were

suitable for describing organic and biological molecules. The DFTB method based on this parameter describes the geometric structure of the system containing elements such as C, H, O, and N in good agreement with the DFT method (Krüger et al., 2005). The dispersion effect was achieved by the Lennard-Jones potential (Lyuben et al., 2005) based on the UFF force field (Rappe et al., 1992). Nosé-Hoover chain thermostat (Martyna et al., 1996) and NVT ensemble were used in all kinetic calculations. The simulation step is 1 fs, the simulation time is not less than 300 ps.

Tunneling and thermal disturbance probabilities

For tunneling probability ($P_{tunneling}$), under the premise of the Born-Oppenheimer approximation, they are calculated based on WKB approximation (Wentzel, 1926; Kramers, 1926; Brillouin, 1926), as following formula (Griffiths, 2005): $P_{tunneling} = Exp\left[-\frac{2}{\hbar}\int_{x_1}^{x_2}\sqrt{2m(V(X)-E_p)}dx\right]$. Among them, m is the reduced mass on the vibration mode corresponding to the imaginary frequency of the TS. This vibration mode contains the main degrees of freedom involved in HAT or depolymerization. E_p is the provided energy assigned to the vibrational mode along the reaction path. V(x) corresponding to the potential energy curve along the reaction path, which is obtained according to the IRC approach (Fukui, 1970; Gonzalez and Schlegel, 1990). This approach has been widely used in the analysis and prediction of a variety of chemical reactions, and shows sufficient reliability (Niu and Hall, 2000; Ziegler and Autschbach, 2005; Zhang et al., 2021; He et al., 2021). Based on the reaction paths, the expression of V(x) is obtained by the Gaussian fitting. x_1 and x_2 are abscissas of the two intersection points for $E = E_p$ and $E = V(x)$. For the thermodynamic model, thermal disturbance probability ($P_{thermal}$) suits the Boltzmann distribution, as following formula: $P_{thermal} = Exp(-\Delta E/k_b T)$ (Landau and Lifshitz, 1980), where ΔE is the difference from E_p to the energy barrier.

QUANTIFICATION AND STATISTICAL ANALYSIS

Analyses and plots were performed with MATLAB and Photoshop.